pss-Header will be provided by the publisher

Photoelectrochemical properties of texture controlled nanostructured α-Fe_2O_3 thin films prepared by AACVD

Asif Ali Tahir [*,1] M.A. Mat-Teridi[,2] and K.G. Upul Wijayantha[3]**

[1] Environment and Sustainability Institute (ESI), University of Exeter, Penryn Campus, Penryn, Cornwall TR10 9FE, UK.
[2] Solar Energy Research Institute, National University of Malaysia, 43600 Bangi, Selangor, Malaysia.
[3]Department of Chemistry, Loughborough University, Loughborough, Leics, LE 11 3TU, UK.

Received ZZZ, revised ZZZ, accepted ZZZ
Published online ZZZ (Dates will be provided by the publisher.)

Keywords : Fe_2O_3, AACVD, photoelectrochemical water-splitting

* Corresponding author: e-mail a.tahir@exeter.ac.uk, Phone: +44 132 625 9320
** e-mail asri@ukm.edu.my, Phone: +60 389 118 580, Fax: +60 389 118 574

Abstract
Nanostructured α-Fe_2O_3 thin film electrodes were deposited by aerosol assisted chemical vapour deposition (AACVD) for photoelectrochemical (PEC) water splitting on conducting glass substrates using 0.1M methanolic solution of $Fe(acac)_3$. The XRD analysis confirmed that the films are highly crystalline α-Fe_2O_3 and free from other iron oxide phases. The highly reproducible electrodes have optical bandgap of ~2.15 eV and exhibit anodic photocurrent. The current-voltage characterization of the electrodes reveals that the photocurrent density strongly dependend on films morphology and deposition temperature. The SEM analysis showed a change in the surface morphology with the change in deposition temperature. The films deposited at 450 °C have nanoporous structures which provide maximum electrode/electrolyte interface. The maximum photocurrent density of 455 μA/cm^2 was acheived at 0.25V vs. Ag/AgCl/3M KCl (~ 1.23 V vs. RHE) and IPCE of 23.6% at 350 nm for the electrode deposited at 450 °C.

1 Introduction

Photoelectrochemical (PEC) water splitting using sunlight is renewable, clean, and cost effective method for solar hydrogen generation [1]. Semiconducting iron oxide (α-Fe_2O_3) is potential candidate material and suitable to employ as a photoelectrode due to its relatively small bandgap energy of ~2.1 eV, which enables it absorb photons up to about 600 nm in the solar spectrum [2]. It is naturally abundant in the Earth's crust, environmentally friendly, non-toxic and substantially less expensive compared to many other known semiconductor materials. α-Fe_2O_3 also has good chemical resistance to corrosion under PEC conditions.

Athough α-Fe_2O_3 has suitable bandgap for efficient absorption of solar spectrum but suffers from poor photoresponse due to high resistivity and charge recombination. The low conductivity and high electron-hole recombination are known to be the key issues of α-Fe_2O_3. Over the past few years, doping and architectural nanostructure control has been the two major approaches adopted to overcome the above issues and then improve PEC properties of hematite. It was suggested that the use of doping agents increase the conductivity of hematite and eventually enhances the PEC properties [3]. A number of dopants such as Si, Pt and Ti have been tested to date [4]. Texture and morphology controlled fabrication of hematite electrode is another apporach, which provides a inimitable opportunity to alter the path of the charge carriers and enhanced electron transport to the back contact to improve the photoconversion efficiency [5]. Quantum confinement is an adequate tool for the upward shift of conduction band edge of semiconductor materials and has been is widely used in solar energy conversion [6]. Recently, research is focused on the fabrication of nanostructured α-Fe_2O_3 with feature size compareable to hole diffusion length to reduce the charge recombination and to improvethe PEC water splitting efficiency of α-Fe_2O_3[**Error! Bookmark not defined.**,7].

Architectural controlled α-Fe_2O_3 nanostructures have been synthesized using various methods, including the hydrothermal method [8], the thermal oxidation method [9], the template based method, anodization methods [10] and microwave-assisted fabrication [11]. Deposition of thin films by various methods has been intensively reported. Among many of them, aerosol-assisted chemical vapour deposition (AACVD) is simple to operate and very versatile. The homogeneity and size of the aerosol droplet can

easily be controlled and tuned by controlling the viscosity of the precursor solution and frequency of the aerosol generator in AACVD process. It also diminishes the volatility requirement of the precursor [12,13]. Moreover, the architectural growth of thin films can easily be controlled by controlling the deposition parameters. Further details of AACVD have been extensively discussed in our recent work [14-16]. In the present work, texture controlled nanostructured hematite thin films were fabricated by using commercially available $Fe(acac)_3$ [acac = 2,4-pentanedione] as the precursor. $Fe(acac)_3$ is highly soluble in most of the organic solvents enabling it an ideal candidate for α-Fe_2O_3 thin films deposition by AACVD. Furthermore, the effect of deposition temperature on the α-Fe_2O_3 electrode texture and PEC performance has been studied.

2 Experimental sections

Nanostructured α-Fe_2O_3 thin films were deposited on fluorine-doped tin oxide (FTO) (TEC 8 Pilkington, 8 Ω/square) substrate by AACVD using [$Fe(acac)_3$] (acac = 2,4-pentanedionate) [17-18]. A 0.1 M methanolic precursor solution was used to generate the aerosol. The carrier gas, air at a rate of 150 mL/min was used and the deposition temperature was varied between 375- 450 ºC by altering the temperature of the hot plate. Each electrode was deposited for a period of 20 min. In addition to the hotplate thermometer, the temperature of FTO substrate surface was also measured using an additional thermocouple externally prior and during deposition. The morphology and nanostructure of thin films were controlled by altering deposition temperature. Bruker AXS D8 Advance X-ray diffractometer with primary monochromatic high-intensity Cu Kα (λ = 1.541 Å) radiation with a PSD detector at the scan step of 0.007° and scan speed of 1 step/s was used to analyze the phase and crystallinity of the deposited films. Surface morphology of thin films was studied by using a field emission gun scanning electron microscope (Leo 1530 VP) at an accelerating voltage of 5 kV, and a working distance of 6 mm.

An electrochemical cell in three-electrode configuration, fitted with a quartz window, was used for photoelectrochemical characterization. All measurements were carried out in 1 M NaOH electrolyte (pH ~ 13.6), using Ag/AgCl/3M KCl as the reference electrode, and a platinum wire as the counter electrode. The potential of the α-Fe_2O_3 working electrode was controlled by a potentiostat (micro-Autolab, type III). The illumination source was an AM 1.5 class A solar simulator (Solar Light 16S – 300 solar simulator). The electrode was illuminated through the electrolyte side and the illumination area was 1 cm^2. For current-voltage characterization, the scan rate was maintained at 0.01 V/s and current density was recorded under light, while manually chopping at regular intervals.

Optical absorption measurements were performed using a Lambda 35 Perkin-Elmer UV−Vis spectrophotometer. The incident photon to electron conversion efficiency (IPCE) was obtained by measuring the incident photon flux using a 75 W Xenon lamp connected to a monochromator (TMc300, Bentham Instruments Ltd). The light was calibrated using a silicon diode. Photocurrent spectra were measured at 0.25 V vs. Ag/AgCl/3MKCl using a combination of a lock-in amplifier (Bentham 485, Bentham Instruments Ltd.) and an in-house built potentiostat. Readings were collected at every 5 nm while the monochromated light was scanned from 320 to 650 nm.

3 Results and discussions

In AACVD, the deposition temperature is a key parameter in controlling the nanostructure of the thin films by switching the heterogeneous and homogeneous chemical reactions in the deposition chamber [19]. In this work, the effect of deposition temperature on nanostructure and PEC performance was investigated and all other parameters such as solvent (methanol), carrier gas flow (150ml/min), precursor solution concentration (0.1M) and deposition time (20 min) are kept constant. Nanostructured α-Fe_2O_3 thin films deposited by AACVD using precursor [$Fe(acac)_3$] are translucent, uniform and adhere strongly on FTO substrate as verified by the scotch tape test. The films deposited above 450 °C poorly adhered to the substrate surface and their PEC performance was negligible. Deposited films were characterized by X-ray diffraction (XRD), FEGSEM, and studied for their optical, photoelectrochemical and incident photon to electron conversion efficiency (IPCE).

The XRD peak pattern of the film deposited at 450 °C on FTO substrate is shown in figure 1 and the XRD diffractogram shows dense SnO_2 diffraction peaks from FTO substrate along with three strong peaks of α-Fe_2O_3 (hematite), specifically (104), (110) and (300) reflections in addition to some weaker peaks corresponding to the (012), (006), (113), (024), (116), and (122) planes. All the observed reflections were closely matched with the standard values of the inter-planar distance *d* for hematite [20] and have been indexed to their respective Miller indices. The volume average mean crystallites size, determined from the broadening of the (104) diffraction peaks by Scherrer formula, is 13 nm and due to the smaller particle size some of the reflection are not strong enough to be observed in the XRD analysis. The higher intensity of the (104) peak indicates that the α-Fe_2O_3 particles are orientated in the (104) direction. The zoomed (104) (fig. 1 inset) peak for all the temperature shows that the crystallinity of the deposited films increases with the increase in deposition temperature. The XRD data for the films deposited at different temperature is normalized to high intensity SnO_2 peak at 37.9°. Martínez et al. [21] reported the deposition of α-Fe_2O_3 films using Fe(β-diketonate) precursor and found that structural properties such as crystallinity and phase are strongly dependent on the deposition temperature. Similarly, Duret et al. deposited films from $Fe(acac)_3$

using a slightly different process (ultrasonic spray pyrolysis) and found Fe_3O_4 phase along with α-Fe_2O_3 [22]. The analysis also proved that no other iron oxide phases is detected in the XRD data suggests that the current method is better to prepare nanostructured α-Fe_2O_3 thin films using $Fe(acac)_3$.

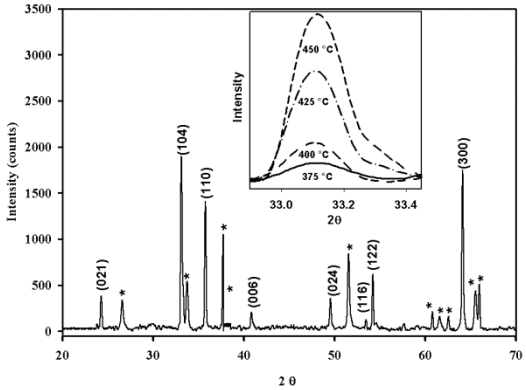

Figure 1: XRD pattern of α-Fe_2O_3 thin film deposited from precursor (**1**) at 450 ºC on an FTO substrate, the peaks marked with (*) corresponds to SnO_2. Inset shows the zoomed (104) peak for all temperatures. The XRD is normalized to high intensity SnO_2 peak at 37.9°.

The optical absorption spectrum has been studied at room temperature in the wavelength range 320-800 nm (figure 2). The recorded optical spectrum was used to calculate the bandgap energy of α-Fe_2O_3 thin films. The optical bandgap (E_g) can be calculated according to following equation

$$\alpha h\nu = A_0 (h\nu - E_g)^n \qquad (1)$$

where α is the absorption coefficient, $h\nu$ is the photon energy in eV, and E_g is the band gap energy in eV. A_o and n are constants, which depend on the kind of electronic transition, n being equal to 1/2 and 2 for allowed direct and indirect transitions, respectively. The inset of figure 2 shows the plot of $(\alpha h\nu)^2$ versus photon energy $h\nu$ for α-Fe_2O_3 film deposited at 450 °C and the bandgap of 2.15 eV was estimated from the intercept by extrapolated linear fit of the Tauc plot to energy axis. The bandgap value is in a good agreement with the previously reported data for the nanostructured α-Fe_2O_3 thin films [23-24].

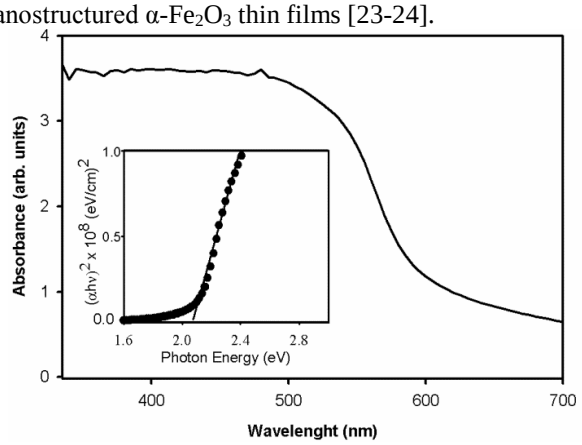

Figure 2: Optical absorption spectrum of α-Fe_2O_3 films deposited at 450 °C. Inset: Tauc plot showing the estimated optical bandgap of 2.15 eV.

The thickness of the films was measured from the SEM cross-section and thickness of the films varies from 0.8-0.9μm. The surface morphology of the film was determined by SEM and figure 3 (inset) shows the SEM images of α-Fe_2O_3 films deposited at 375- 450 ºC. The SEM image of the film deposited at 375 ºC shows small nanoparticles sintered together to form a compact morphology. A close view of SEM images showed the formation of some plate-like features, which are identifiable in the film deposited at 400 ºC. At 400 ºC the small particles coagulate to form large agglomerates and the plate-like features start to form resulting in an increase of the porosity. The film deposited at 425 ºC has a very distinct morphology with clearly visible nanoplates. These nanoplates combine together to form flower-like nanostructures and the formation of them increases the electrode porosity further. Continuation of raising the deposition temperature to 450 ºC completely changes the morphology of the films. Such films exhibit a very high internal surface area and the average grain size observed in SEM is larger than those estimated from the Scherer's equation. The agglomerates/clusters are relatively smaller than those of the films deposited at relatively lower temperatures and a change in the architecture of interconnected pores is also clearly evident. Smaller crystallite size along with less agglomeration facilitates the formation of hematite thin films with the size of the particles more compatible to the literature reported hole diffusion length for hematite structure [**Error! Bookmark not defined.**].

Growth of films with range of structure, texture and morphology with altration of deposition temperature can be explained on the basis of heterogeneous and homogeneous nucleation pathway of CVD process [25]. If the vaporized precursor undergoes decomposition in the gas phase it is called homogeneous reaction/nucleation. However, if the vaporized precursor adsorbed on the heated substrate and then decomposes it is referred to as heterogeneous reaction/nucleation. The formation of thin films in the AACVD process is the result of homogeneous or heterogeneous reaction or a combination of both. Therefore, the nature of reaction is directly responsible for the morphology, structure and composition of the thin films [26]. By keeping all the other AACVD parameters constant, the type of nucleation reaction (homogeneous or heterogeneous) can easily be controlled by the substrate temperature. In the current work, this phenomenon was exploited to deposit α-Fe_2O_3 thin films with diverse texture and nanostructure by altering the deposition temperature. We attribute the change in morphology with the increase in temperature to the gradual shift of nucleation from heterogeneous to homogeneous. The mechnisim of

AACVD deposition and effect of homogeneous or heterogeneous nucleation on the texture and morphology of thin films has been discussed in detail elsewhere. [18, 27]

The photoelectrochemical performance of nanostructured α-Fe_2O_3 films was studied by recording the photocurrent density as a function of applied voltage (figure 3). The steady-state photocurrent density increased with the increase of deposition temperature. The photocurrent behaviour have also been studied under chopped light and for comparison, the steady-state *J*-V plot was superimposed on the transient plot in each case. Steady-state and transient *J*-V plots agree well for all electrodes. Generally, dark current starts at about 0.6 V for all the electrodes in 1 M NaOH electrolyte. The amount of dark current also decreased with the increase of deposition temperature. For all electrodes, photocurrent increased rapidly with the applied potential. Figure 3 shows a maximum photocurrent of 455 μAcm^{-2} at 0.25 V for the electrode deposited at 450 °C. The photocurrent maximum observed for electrode prepared at 450 °C can be interpreted in terms of large active surface area (hence the large effective semiconductor/electrolyte interface), which possibly associated with the enhanced charge transfer at the interface. The separation of photogenerated carriers within the width of the space charge layer becomes a key factor, which seems to be more pronounced in the case of the electrodes deposited at 450 °C. This increase can also be atributed to high crystallinity of the films as confirmed by the XRD analysis. The electrode prepared at 375 °C has the weakest PEC performance with recombination features in the photocurrent transient responses close to photocurrent onset region presumably due to its compact morphology. With the increase of deposition temperature, the electrode structure became more porous. The nanoporous structure (at 425 °C and 450 °C) has the advantage as it contains α-Fe_2O_3 nanostructures which provide better electrode/electrolye interface for rapid charge transfer. Such nanostructures offer very short distance required for the photogenerated holes to reach the electrolyte interface thereby suppressing the recombining. The PEC performance of films deposited at 450 °C are comparable to our previouse α-Fe_2O_3 photoelectrode deposited using a metal-organic complex [17]. This increase the rate of PEC water splitting by holes despite that the hole diffusion length is in the order of 2-4 nm [**Error! Bookmark not defined.**]. Further work is need to controll the particle size of hematite nanostructures in the same order of hole-diffusion length to enhance the PEC performance.

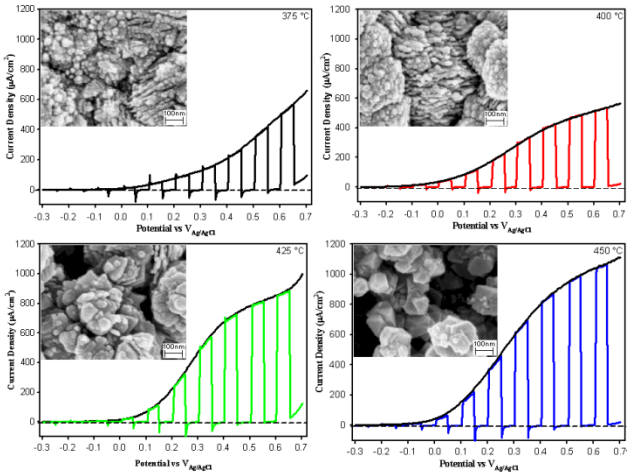

Figure 3. *J*-V curves for α-Fe_2O_3 electrodes deposited at different deposition temperatures. Inset shows the high resolution SEM of respective electrodes.

In order to further explor the influence of temperature on PEC performance of the films deposited at different temperatures, the incident photon to electron conversion efficiency (IPCE) measurements were conducted at different wavelengths and at 0.25 V vs. Ag/AgCl/3MKCl. As shown in figure 4, the IPCE of electrodes are almost similar at wavelengths greater than 610 nm which is outside the absorption threshold of α-Fe_2O_3. The IPCE increases with the increase in deposition temperature after the absorption threshold. The maximum efficiency of 11.5, 13.5, 19.7 and 23.6% was attained at 345 nm for the electrodes deposited at 375, 400, 425 and 450 °C respectively. The high efficiency values at short wavelengths are understood by the fact that the light diffusion depth at short wavelengths is low and these high energy photons are absorbed in the vicinity of the surface of the film. The closer the photogenerated holes to the surface, the more efficient the collection of holes at the surface of the electrode as the holes have to diffuse through a shorter path to reach the surface of the electrode. As the hole diffusion length in hematite is very small, therefore reducing the particle size and increase the electrode/electrolyte interface could contribute to better hole diffusion and more efficient charge separation at the surface. The increase in the IPCE with increase in the deposition temperature is attributed to the higher active surface area observed in the SEM topography (figure 3).

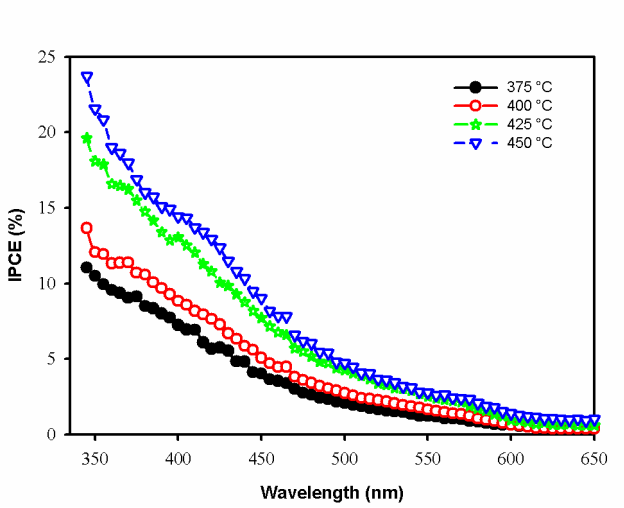

Figure 4: IPCE spectra as a function of wavelength at 0.25 V vs. Ag/AgCl/3MKCl for the α-Fe_2O_3 electrodes deposited at 375-450 °C.

4 Conclusions

Nanostructured α-Fe_2O_3 thin films electrodes were deposited by AACVD on FTO conducting glass substrates using 0.1M methanolic solution of $Fe(acac)_3$. A range of thin film electrode textures, from compact to nanoporous, were achieved by controlling the deposition temperature. The dramatic change of electrode texture was attributed to the heterogeneous and homogeneous nature of AACVD reaction that taken place inside the reaction chamber. The robust thin film electrodes were studied for materials, optical, electrical and photoelectrochemical properties. The XRD analysis showed that the crystalline phase of the thin film material is α-Fe_2O_3. The best photocurrent density of 455 μA/cm^2 (at 0.23V vs. Ag/AgCl/3M KCl) was recorded for the nanocrystalline α-Fe_2O_3 electrode prepared at the deposition temperature of 450 °C. The same electrode was shown an IPCE of 23.6% at the same bias at 350 nm, which was the highest recorded IPCE value for the α-Fe_2O_3 electrode series investigated in this study. The nanoporous flower-like structure deposited at 425 °C and 450 °C shows better performance by absorbing more visible light and reducing recombination due to short distance required for the photogenerated holes to reach the electrolyte interface. This work shows that the photoelectrochemical performance of hematite electrodes can be enhanced by controlling the texture of α-Fe_2O_3 and further work is needed to control the individual particle size analogous to the hole diffusion length of the α-Fe_2O_3 to enhance the performance of α-Fe_2O_3 photoelectrodes.

Acknowledgements This work was supported by the EPSRC award EP/F057342/1 and MOHE award FRGS/2/2013/TK06/UKM/03/1.

References

[1] M. Grätzel, Nature 414, 338 (2001)
[2] S. K. Mohapatra, S. E. John, S. Banerjee, M. Misra, Chem. Mater. 21, 3048 (2009).
[3] I. Cesar, A. Kay, J. A. G. Martinez, M. Grätzel, J. Am. Chem. Soc. 128, 4582 (2006).
[4] J. A. Glasscock, P. R. F. Barnes, I. C. Plumb, N. Savvides, J. Phys. Chem. C 111, 16477 (2007).
[5] N. Beermann, L. Vayssieres, S.-E. Lindquist, A. Hagfeldt, J. Electrochem. Soc. 147, 2456 (2000).
[6] L. Vayssieres, C. Sathe, S. M. Butorin, D. K. Shuh, J. Nordgren, J. H. Guo, Adv. Mater. 17, 2320 (2005).
[7] H. E. Prakasam, O. K. Varghese, M. Paulose, G. K. Mor, C. A. Grimes, Nanotechnology 17, 4285 (2006).
[8] C. J. Jia, L. D. Sun, Z. G. Yan, L. P. You, F. Luo, X. D. Han, Y. C. Pang, Z. Zhang, C. H. Yan, Angew. Chem., Int. Ed. 44, 4328 (2005).
[9] T. J. LaTempa, X. Feng, M. Paulose, and C. A. Grimes, J. Phys. Chem. C 113, 16293 (2009).
[10] S. K. Mohapatra, S. Banerjee, M. Misra, Nanotechnology 19, 315601 (2008).
[11] S. Saremi-Yarahmadi, B. Vaidhyanathan, K. G. U. Wijayantha, Inter. J. Hydrogen Energy, 35, 10155 (2010).
[12] W. B. Cross, I. P. Parkin, S. A. O'Neill, P. A. Williams, M. F. Mahon, K. C. Molloy, Chem. Mater. 15, 2786 (2003).
[13] A. A. Tahir, M. Mazhar, M. Hamid, K. G. U. Wijayantha, K. C. Molloy, Dalton Trans. 3674 (2009).
[14] P. Hiralal, H. E. Unalan, K. G. U. Wijayantha, A. Kursumovic, D. Jefferson, J. L. MacManus-Driscoll, G. A. J. Amaratunga, Nanotechnology 19, 455608 (2008).
[15] S. Saremi-Yarahmadi, A. A. Tahir, B. Vaidhyanathan, K. G. U. Wijayantha, Mater. Lett. 63, 523 (2009).
[16] S. Saremi-Yarahmadi, A. A. Tahir, K. G. U. Wijayantha, B. Vaidhyanathan, J. Phys. Chem. C113, 4768 (2009).
[17] A. A. Tahir, K. G. U. Wijayantha, S. Saremi-Yarahmadi, M. Mazhar, V. McKee, Chem. Mater. 21, 3763 (2009).
[18] A. A. Tahir, K. G. U. Wijayantha, M. Mazhar, V. McKee, Thin Solid Films, 518, 3664 (2010).
[19] A. A. Tahir, M. A. Ehsan, M. Mazhar, K. G. U. Wijayantha, M. Zeller, A. D. Hunter, Chem. Mater. 22,5084 (2010).
[20] ICDD card No. 00-033-0664. Natl. Bur. Stand. (U. S.) Monogr. 25, 37 (1981).
[21] A. Martinez, J. Pena, M. Labeau, J. M. Gonzalez-Calbet, M. Vallet-Regi, J. Mater. Res. 10, 1307 (1995).
[22] A. Duret, Grätzel, M., J. Phys. Chem. B, 109, 17184 (2005).
[23] J. D. Desai, H. M. Pathan, S-K. Min, K-D. Jung, O-S. Joo, App. Sur. Sc. 252, 8039 (2006).
[24] J. D . Desai, H. M. Pathan, S-K. Min, K-D. Jung, O-S. Joo, Semicond. Sci. Technol. 20, 705 (2005).
[25] X. Hou, and K.-L. Choy, Chem. Vap. Deposition 12, 583 (2006).
[26] T. T. Kodas, and M. J. Hampden-Smith, The Chemistry of Metal CVD; VCH: Weinheim, (1994)
[27] A. A. Tahir, H. A. Burch, K. G. U. Wijayantha, B. G. Pollet Inter. J. Hydrogen Energy, 38, 4315 (2013).